

Communication

## Efficient Hydrogen Production from Methanol Using A Single-Site Pt1/CeO2 Catalyst

Lu-ning Chen, Kai-Peng Hou, Yi-Sheng Liu, Zhi-yuan Qi, Qi Zheng, Yi-Hsien Lu, Jia-yu Chen, Jeng-Lung Chen, Chih-Wen Pao, Shuo-bo Wang, Yao-bin Li, Shao-hua Xie, Fu-Dong Liu, David Prendergast, Leonard E Klebanoff, Vitalie Stavila, Mark D. Allendorf, Jinghua Guo, Lan-Sun Zheng, Ji Su, and Gabor A. Somorjai

*J. Am. Chem. Soc.*, **Just Accepted Manuscript** • DOI: 10.1021/jacs.9b09431 • Publication Date (Web): 24 Oct 2019

Downloaded from pubs.acs.org on October 25, 2019

### Just Accepted

"Just Accepted" manuscripts have been peer-reviewed and accepted for publication. They are posted online prior to technical editing, formatting for publication and author proofing. The American Chemical Society provides "Just Accepted" as a service to the research community to expedite the dissemination of scientific material as soon as possible after acceptance. "Just Accepted" manuscripts appear in full in PDF format accompanied by an HTML abstract. "Just Accepted" manuscripts have been fully peer reviewed, but should not be considered the official version of record. They are citable by the Digital Object Identifier (DOI®). "Just Accepted" is an optional service offered to authors. Therefore, the "Just Accepted" Web site may not include all articles that will be published in the journal. After a manuscript is technically edited and formatted, it will be removed from the "Just Accepted" Web site and published as an ASAP article. Note that technical editing may introduce minor changes to the manuscript text and/or graphics which could affect content, and all legal disclaimers and ethical guidelines that apply to the journal pertain. ACS cannot be held responsible for errors or consequences arising from the use of information contained in these "Just Accepted" manuscripts.

# Efficient Hydrogen Production from Methanol Using A Single-Site Pt<sub>1</sub>/CeO<sub>2</sub> Catalyst

Lu-Ning Chen,<sup>1,2</sup> Kai-Peng Hou,<sup>1,3</sup> Yi-Sheng Liu,<sup>5</sup> Zhi-Yuan Qi,<sup>1</sup> Qi Zheng,<sup>1</sup> Yi-Hsien Lu,<sup>1</sup> Jia-Yu Chen,<sup>2</sup> Jeng-Lung Chen,<sup>6</sup> Chih-Wen Pao,<sup>6</sup> Shuo-Bo Wang,<sup>1</sup> Yao-Bin Li,<sup>7</sup> Shao-Hua Xie,<sup>8</sup> Fu-Dong Liu,<sup>8</sup> David Prendergast,<sup>4</sup> Leonard E. Klebanoff,<sup>9</sup> Vitalie Stavila,<sup>9</sup> Mark D. Allendorf,<sup>9</sup> Jinghua Guo,<sup>5</sup> Lan-Sun Zheng,<sup>2</sup> Ji Su,<sup>\*,1,4</sup> Gabor A. Somorjai<sup>\*,1,3</sup>

<sup>1</sup> Materials Sciences Division, <sup>4</sup> Molecular Foundry, Material Science Division, <sup>5</sup> Advanced Light Source, Lawrence Berkeley National Laboratory, Berkeley, California 94720, United States.

<sup>2</sup> State Key Laboratory of Physical Chemistry of Solid Surfaces, Collaborative Innovation Center of Chemistry for Energy Materials, and Department of Chemistry, College of Chemistry and Chemical Engineering, Xiamen University, Xiamen 361005, China.

<sup>3</sup> Department of Chemistry, University of California-Berkeley, Berkeley, California 94720, United States.

<sup>6</sup> National Synchrotron Radiation Research Center, Science-Based Industrial Park Hsinchu 30076, Taiwan.

<sup>7</sup> Institute of Urban Environment, Chinese Academy of Sciences, Xiamen 361021, China.

<sup>8</sup> Department of Civil, Environmental, and Construction Engineering, Catalysis Cluster for Renewable Energy and Chemical Transformations (REACT), Nano-Science Technology Center (NSTC), University of Central Florida, Orlando, Florida, 32916, United States.

<sup>9</sup> Sandia National Laboratories, Livermore, CA 94551, United States.

## Supporting Information Placeholder

**ABSTRACT:** Hydrogen is regarded as an attractive alternative energy carrier due to its high gravimetric energy density and only water production upon combustion. However, due to its low volumetric energy density, there are still some challenges in practical hydrogen storage and transportation. In the last decade, using chemical bonds of liquid organic molecules as hydrogen carriers to generate hydrogen in situ provided a feasible method to potentially solve this problem. Research efforts on liquid organic hydrogen carriers (LOHCs) seek practical carrier systems and advanced catalytic materials that have the potential to reduce costs, increase reaction rate, and provide a more efficient catalytic hydrogen generation/storage process. In this work, we used methanol as a hydrogen carrier to release hydrogen in situ with the single-site Pt<sub>1</sub>/CeO<sub>2</sub> catalyst. Moreover, in this reaction, compared with traditional nanoparticle catalysts, the single site catalyst displays excellent hydrogen generation efficiency, 40 times higher than 2.5 nm Pt/CeO<sub>2</sub> sample, and 800 times higher compared to 7.0 nm Pt/CeO<sub>2</sub> sample. This in-depth study highlights the benefits of single-site catalysts and paves the way for further rational design of highly efficient catalysts for sustainable energy storage applications.

In order to reduce atmospheric pollution and greenhouse gas emission, developing clean energy sources has attracted growing interest. Among them, hydrogen is desirable as an alternative clean fuel, because it can be converted efficiently to energy without producing toxic products or greenhouse gases.<sup>[1]</sup> Nowadays, hydrogen is widely used in different fields, especially in polymer electrolyte membrane fuel cells (PEMFCs) due to its high gravimetric energy density (120 MJ/kg).<sup>[2]</sup> In contrast to other hydrogen transportation and storage approaches, such as compressed gas, or solid-state storage in metal hydrides and metal-organic frameworks (MOFs),<sup>[3,4]</sup> the liquid organic hydrogen carriers (LOHCs) concept involves transportation of hydrogen in liquids, and generating hydrogen in situ by breaking chemical bonds, often times in the presence of a catalyst.<sup>[5,6]</sup> There are advantages to transporting and handling liquids, such as added safety, greater energy density, and possibility of utilizing the existing gasoline and oil infrastructure and reduced costs overall.

For practical applications, a key factor is to look for an appropriate liquid organic molecule as hydrogen carrier.<sup>[7]</sup> Compared to other liquid organic molecules, methanol is a suitable molecule with high hydrogen gravimetric density. Moreover, methanol is relatively inexpensive and can be manufactured from a variety of sources which can

transformed from some harmful gas or greenhouse gases like CO, CO<sub>2</sub> and CH<sub>4</sub>.<sup>[8,9]</sup> In addition, seeking an efficient catalyst to in situ generate large quantity of hydrogen in a short time is another significant factor. In catalytic hydrogen production, the traditional support metal catalysts typically need high temperature and high metal loadings to achieve a relatively good catalytic performance.<sup>[10]</sup> As previously studied, the size of metal particles is critically important in determining the performance of metal supported catalysts in many catalytic reactions.<sup>[11,12]</sup> Moreover, the ultimate small-size limit for particles is the single-site catalyst with isolated single metal sites dispersed on solid supports. With maximum atom-utilization efficiency (100 %), high specific activity and unique properties can be realized, single-site catalysts are emerging as a new frontier in catalytic science.<sup>[13-17]</sup>

Herein, we successfully synthesized single-site Pt<sub>1</sub>/CeO<sub>2</sub> catalyst with single Pt sites anchored on porous CeO<sub>2</sub> supported by a modified ascorbic acid (AA)-assisted reduction route.<sup>[18-19]</sup> In the catalytic hydrogen production from methanol, compared with traditional Pt nanoparticles catalysts (2.5 nm Pt/CeO<sub>2</sub>, 7.0 nm Pt/CeO<sub>2</sub>), this single-site catalyst performed high activity at relative low temperature with low Pt loading. Additionally, this single-site catalyst can be applied to other alcohol catalytic hydrogen production.

In our study, porous CeO<sub>2</sub> nanorods (Figure S1) were chosen as the support to anchor Pt single atoms by AA-assisted reduction route, named Pt<sub>1</sub>/CeO<sub>2</sub>. Meanwhile, we also synthesized Pt nanoparticles with different sizes and loadings on CeO<sub>2</sub> by pre-synthesizing Pt nanoparticles and mixing them with CeO<sub>2</sub>, and the capping agent on Pt surface was further removed by UV-ozone treatment.<sup>[20,21]</sup> The loading amounts of Pt are both were about 1% wt. For convenience, the Pt nanoparticles loaded on CeO<sub>2</sub> are named 2.5 nm Pt/CeO<sub>2</sub> and 7.0 nm Pt/CeO<sub>2</sub>, whose sizes are determined by TEM measurement (Figure S2).

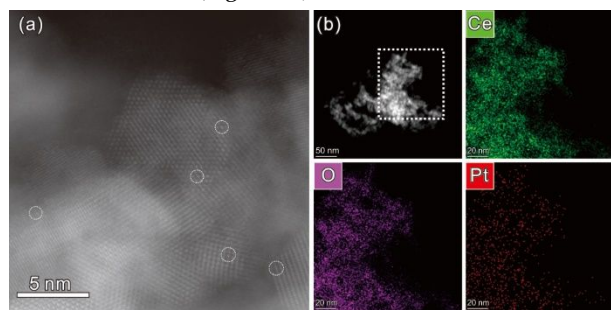


Figure 1. (a) Cs-corrected high-angle annular dark-field scanning transmission electron microscopy (HAADF-STEM) images of Pt<sub>1</sub>/CeO<sub>2</sub> catalyst, the brighter dots cycled are Pt single sites, (b) HAADF-STEM and corresponding elemental mappings images of Pt<sub>1</sub>/CeO<sub>2</sub> catalyst.

The loading status of Pt loading on CeO<sub>2</sub> catalysts were compared by powder X-ray diffraction (XRD) and transmission electron microscope (TEM). From the XRD data, there are no diffraction peaks observable from metallic Pt for all the three catalysts due to the low Pt content and small Pt particle sizes (Figure S3). In the bright-field TEM images of 2.5 nm Pt/CeO<sub>2</sub> and 7.0 nm Pt/CeO<sub>2</sub>, the Pt nanoparticles are uniformly dispersed on CeO<sub>2</sub> nanorods (Figure S4b, c). However, for Pt<sub>1</sub>/CeO<sub>2</sub> catalyst there is no apparent difference compared to original CeO<sub>2</sub> nanorods (Figure S1a), with no metallic clusters or particles being observed (Figure S4a).

Moreover, from corresponding elemental mapping, the Pt signals are uniformly distributed overall CeO<sub>2</sub> nanorods (Figure 1b). In order to further confirmed the actual Pt loading information on CeO<sub>2</sub>, the HAADF-STEM measurement was applied. As shown in Figure 1a, the Pt catalytic sites were atomically dispersed throughout the porous CeO<sub>2</sub>, and the actual Pt content was 0.15%.

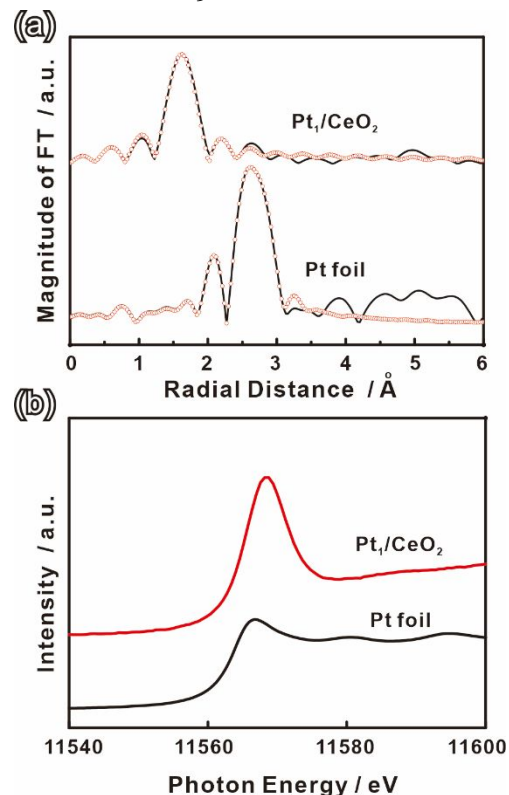


Figure 2. (a)  $k^3$ -weighted Fourier transform EXAFS spectra and (b) normalized XANES spectra of Pt<sub>1</sub>/CeO<sub>2</sub> and bulk Pt foil at the Pt L<sub>3</sub>-edge. The red hollow points are fitting results.

Extended X-ray absorption fine structure (EXAFS) spectra were acquired to provide the valence and coordinated structure of single-site Pt<sub>1</sub>/CeO<sub>2</sub> catalyst. Compared with bulk Pt foil there is no nearest neighbor Pt-Pt bond observed in the single-site Pt<sub>1</sub>/CeO<sub>2</sub> catalyst, while the notable peak observed between 1 to 2 Å is attributed to contribution of Pt-O bond (Figure 2). The Pt dispersion states for the three samples are further verified by in situ DRIFTS of CO absorption and desorption (Figure S5). For the single-site Pt<sub>1</sub>/CeO<sub>2</sub> catalyst, three bands are observed, of which the bands at 2171 and 2117 cm<sup>-1</sup> are attributed to the CO gas, while that at 2090 cm<sup>-1</sup> are attributed to the linearly (on-top) bonded CO on Pt ionic species.<sup>[13,18]</sup> However, for 2.5 nm Pt/CeO<sub>2</sub> and 7.0 nm Pt/CeO<sub>2</sub> there is another band on at 2050 cm<sup>-1</sup> due to the linear absorbance of CO on the small sized Pt nanoparticles on CeO<sub>2</sub>.<sup>[13,22]</sup>

In the direct methanol catalytic hydrogen production, compared with traditional Pt nanoparticles (2.5 nm Pt/CeO<sub>2</sub> and 7.0 nm Pt/CeO<sub>2</sub>), the single-site Pt loaded on CeO<sub>2</sub> (Pt<sub>1</sub>/CeO<sub>2</sub>) displayed excellent catalytic performance (Figure 3a). At the temperature below 150 °C, both the Pt single-site and Pt nanoparticle catalysts have no obviously catalytic activity. As the temperature was increased to above 150 °C, both the formation of hydrogen and carbon monoxide were detected. Further increasing the reaction temperature, more

methanol was converted to hydrogen and carbon monoxide. Moreover, due to the size effect, the single-site  $\text{Pt}_1/\text{CeO}_2$  catalyst performed with higher activity for hydrogen production from methanol than the 7.0 nm  $\text{Pt}/\text{CeO}_2$  and 2.5 nm  $\text{Pt}/\text{CeO}_2$  counterparts. The turnover frequency (TOF) of  $\text{Pt}_1/\text{CeO}_2$  catalyst is much higher than traditional Pt nanoparticle, up to  $12500 \text{ h}^{-1}$  at  $300^\circ\text{C}$ , which is 40 times that of 2.5 nm  $\text{Pt}/\text{CeO}_2$  and almost 800 times that of 7.0 nm  $\text{Pt}/\text{CeO}_2$ . Furthermore, the single-site  $\text{Pt}_1/\text{CeO}_2$  sample is highly stable: after reaction at  $300^\circ\text{C}$  for 120 hours, the catalyst keeps more than 90% of its best activity (Figure 3b). The decrease of activity at initial times is due to the loss of unstable absorb Pt sites on  $\text{CeO}_2$  surface. The Pt content of  $\text{Pt}_1/\text{CeO}_2$  catalyst decreased to 0.13% after the first 10 hours of reaction and thereafter remains almost the same after 120 hours reaction. After long-time reaction, there is still no Pt-Pt bond detected by EXAFS (Figure S6) indicating there is no agglomeration happened even after long-time reaction at  $300^\circ\text{C}$ .

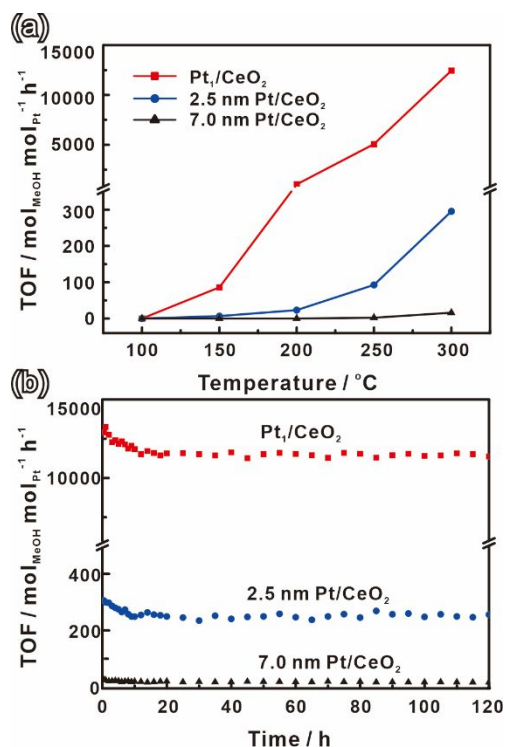


Figure 3. (a) Turnover frequency (TOF) of hydrogen production from methanol in terms of methanol conversion per Pt site of  $\text{Pt}_1/\text{CeO}_2$ , 2.5 nm  $\text{Pt}/\text{CeO}_2$  and 7.0 nm  $\text{Pt}/\text{CeO}_2$ , at different temperatures. (b) the stability  $\text{Pt}_1/\text{CeO}_2$ , 2.5 nm  $\text{Pt}/\text{CeO}_2$  and 7.0 nm  $\text{Pt}/\text{CeO}_2$  at reaction condition at  $300^\circ\text{C}$ .

The dehydrogenation mechanism of methanol on the Pt surface have been experimentally examined using advanced techniques such as: TPD, EELS, IR, UPS, and AES. The dehydrogenation mechanism has also been examined via DFT theoretical simulation.<sup>[10,23-25]</sup> These results indicate that, at low temperature, methanol molecularly absorbs at the surface of Pt and then decomposes to form methoxy species by breaking the O-H bond. Then successively, the three C-H bonds will be broken up and generate the final products  $\text{CO}_{\text{ads}}$  and  $\text{H}_{\text{ads}}$ . Importantly, both experimental and computational results demonstrated that smaller Pt nanoparticle size favor the methanol dehydrogenation due to the energy barriers of

both O-H and C-H bond cleavage, much lower on the defects and steps of the Pt surface.

We also measured the catalytic hydrogen production performance of single-site  $\text{Pt}_1/\text{CeO}_2$  catalyst as a function of the methanol feeding rate (Figure S7). At lower methanol feeding rate, the conversion of methanol is higher. When the feeding rate is 0.01 ml/min, methanol can totally convert to hydrogen, which proves that this catalyst can be applied in practical applications. As the feeding rate of methanol is increased, the TOF increases as well. The TOF is almost  $15000 \text{ h}^{-1}$  at the feeding rate of 0.1 ml/min, illustrating the high catalytic activity of  $\text{Pt}_1/\text{CeO}_2$  catalyst. We as well synthesized a series of  $\text{Pt}_1/\text{CeO}_2$  catalysts with different Pt content by controlling the feeding amount of Pt precursor (Figure S8a). And all the  $\text{Pt}/\text{CeO}_2$  catalysts performed high activity in methanol dehydrogenation. However, the TOF decrease of  $\text{Pt}/\text{CeO}_2$ -0.3% and 0.45%, due to Pt agglomeration at higher content (Figure S8b). No hydrogenation formation was detected with pure  $\text{CeO}_2$  nanorods without Pt loading, indicating that the active site is Pt instead of  $\text{CeO}_2$ .

Single-site catalysts are typically systems where the activity of a central metal atom/atoms relies on interactions with heteroatomic ligands (such as N or O bridge) that anchor it to metal atoms of the substrate. The electronic structure and reactivity of Pt are very sensitive to support. In our study, the Pt element valence states was proven to be another factor influencing its catalytic activity. The Pt and Ce valence states of  $\text{Pt}_1/\text{CeO}_2$ , 2.5 nm  $\text{Pt}/\text{CeO}_2$  and 7.0 nm  $\text{Pt}/\text{CeO}_2$  are further confirmed by XPS analysis (Figure S9). Importantly, for the Pt 4f XPS spectra, the binding energies of Pt  $4f_{7/2}$  and  $4f_{5/2}$  in  $\text{Pt}_1/\text{CeO}_2$  are close to  $\text{Pt}^{2+}$  species, indicating that Pt single-site supported on  $\text{CeO}_2$  are oxidized owing to the electron transfer Pt to  $\text{CeO}_2$ .<sup>[26]</sup> Interestingly, the Pt species of 2.5 nm  $\text{Pt}/\text{CeO}_2$  and 7.0 nm  $\text{Pt}/\text{CeO}_2$  are mainly metallic Pt. The previous reports have certified that the Pt-CO bonding energy of CO absorption on positive Pt species is lower than on metallic Pt.<sup>[19,27]</sup> Thus, for the methanol dehydrogenation process, as the  $\text{CO}_{\text{ads}}$  species forms, it is much easier to desorb CO from positive Pt sites in  $\text{Pt}_1/\text{CeO}_2$  than the metallic Pt sites of other two catalysts (Figure S10). Therefore, the size effect and valence states of Pt may explain the relative catalytic activity of these catalyst samples, with activity ordered as: single-site  $\text{Pt}_1/\text{CeO}_2 \gg 2.5 \text{ nm } \text{Pt}/\text{CeO}_2 > 7.0 \text{ nm } \text{Pt}/\text{CeO}_2$ .

The single-site  $\text{Pt}_1/\text{CeO}_2$  also performed excellent catalytic activity in hydrogen production from other alcohols, namely ethanol, 1-propanol, isopropanol, 1-butanol, and benzyl alcohol (Figure 4). The proposed mechanism of the alcohol dehydrogenation process includes several steps. First, the alcohol molecules absorb on Pt sites and form  $\text{R}_1\text{R}_2\text{CHO}_{\text{ads}}$  by breaking O-H bond, then dehydrogenation into  $\text{R}_1\text{R}_2\text{CO}_{\text{ads}}$ . As for methanol, after formaldehyde ( $\text{CH}_2\text{O}$ ) intermediate is formed, it will further dehydrogenate to yield formyl ( $\text{CHO}$ ) and carbon monoxide ( $\text{CO}$ ).<sup>[10,24,25]</sup> Hence, compared to other alcohols, all the hydrogen in methanol can be released to generate two molecules of  $\text{H}_2$  and leave CO behind. For other longer chain alcohols, after aldehydes or ketones formed, more energy is needed for additional dehydrogenation steps. Moreover, for primary alcohols, the activity of substrates is decreased with the growth of carbon chain, and after transformation to corresponding aldehydes, some C-C bonds will be cleaved to form CO and alkanes. Besides, the hydrogen



production from benzyl alcohol and isopropanol is higher, owing to their first dehydrogenated products are more stable.

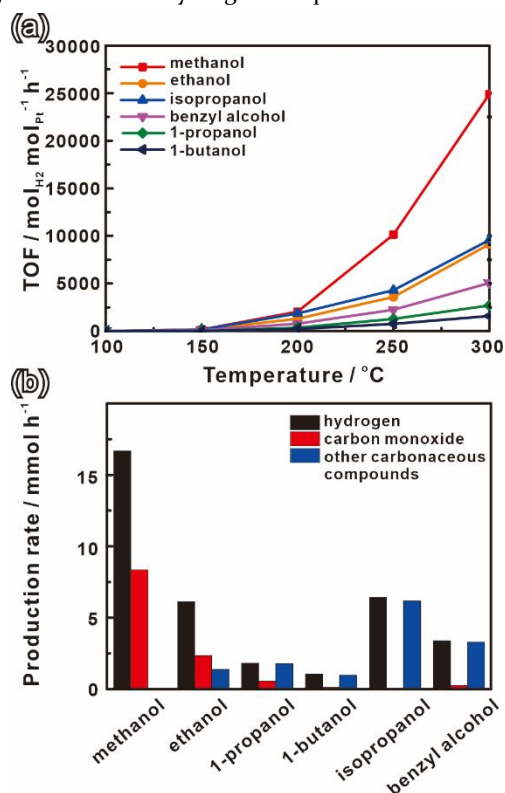


Figure 4. (a) Turnover frequency (TOF) of hydrogen production from different alcohol in terms of hydrogen production per Pt site of  $\text{Pt}_1/\text{CeO}_2$  at different temperature. (b) Products diffusion of different alcohol at 300  $^{\circ}\text{C}$  by  $\text{Pt}_1/\text{CeO}_2$  catalyst.

In summary, a well-defined single-site  $\text{Pt}_1/\text{CeO}_2$  catalyst was developed and its catalytic performance was evaluated for hydrogen generation from methanol. Importantly, compared to the  $\text{Pt}/\text{CeO}_2$  nanoparticle catalysts (2.5 nm  $\text{Pt}/\text{CeO}_2$  and 7.0  $\text{Pt}/\text{CeO}_2$ ), the single-site catalyst  $\text{Pt}_1/\text{CeO}_2$ , exhibited reaction rates that are 40 and 800 times higher, respectively. Moreover, beside the methanol, this single-site catalyst performed high efficiency in other liquid alcohol hydrogen production. Ultimately, this in-depth study highlights the benefits of single-site catalyst and paves the way for further rational design of highly efficient catalysts for hydrogen production.

## ASSOCIATED CONTENT

### Supporting Information

This material is available free of charge via the Internet at <http://pubs.acs.org>.

Experimental details, characterization data and partial catalytic data, including the synthesis of catalysts, the characterization of  $\text{CeO}_2$  support and catalysts, the characterization of catalyst after reaction, and the catalytic result of some control tests.

## AUTHOR INFORMATION

### Corresponding Author

[jisu@lbl.gov](mailto:jisu@lbl.gov)

[somorjai@berkeley.edu](mailto:somorjai@berkeley.edu)

## Notes

The authors declare no competing financial interests.

## ACKNOWLEDGMENT

This work was supported by the Hydrogen Materials Advanced Research Consortium (HyMARC), established as part of the Energy Materials Network by the U.S. Department of Energy, Office of Energy Efficiency and Renewable Energy, Fuel Cell Technologies Office, under Contract Number DE-AC02-05CH11231. This research used resources of the Advanced Light Source, which is a DOE Office of Science User Facility under contract no. DE-AC02-05CH11231. L. Chen, Y. Liu, J. Guo, D. Prendergast and J. Su were supported by a User Project at The Molecular Foundry at Lawrence Berkeley National Laboratory, which is supported by the Office of Science of the U.S. Department of Energy under contract no. DE-AC02-05CH11231. Sandia National Laboratories is a multi-mission laboratory managed and operated by National Technology and Engineering Solutions of Sandia, LLC., a wholly owned subsidiary of Honeywell International, Inc., for the U.S. Department of Energy's National Nuclear Security Administration under Contract No. DE-NA-0003525. L. Chen and S. Wang thank the China Scholarship Council (CSC) for financial support.

## REFERENCES

- (1) Schultz, M. G.; Diehl, T.; Brasseur, G. P.; Zittel, W. Air Pollution and Climate-Forcing Impacts of a Global Hydrogen Economy. *Science* **2003**, *302*, 624.
- (2) Steele, B. C. H.; Heinzel, A. Materials for fuel-cell technologies. *Nature* **2001**, *414*, 345.
- (3) Schneemann, A.; White, J. L.; Kang, S.Y.; Jeong, S.; Wan, L. F.; Cho, E. S.; Heo, T. W.; Prendergast, D.; Urban, J. J.; Wood, B. C.; Allendorf, M. D.; Stavila, V. Nanostructured metal hydrides for hydrogen storage. *Chem. Rev.*, **2018**, *118*, 10775.
- (4) Allendorf, M.D.; Hulvey, Z.; Gennett, T.; Ahmed, A.; Autrey, T.; Camp, J.; Cho, E. S.; Furukawa, H.; Haranczyk, M.; Head-Gordon, M.; Jeong, S.; Karkamkar, A.; Liu, D.-J.; Long, J. R.; Meihaus, K. R.; Nayyar, I. H.; Nazarov, R.; Siegel, D. J.; Stavila, V.; Urban, J. J. Veccham S. P.; Wood, B.C. An assessment of strategies for the development of solid-state adsorbents for vehicular hydrogen storage. *Energy Environ. Sci.*, **2018**, *11*, 2784.
- (5) Preuster, P.; Papp, C.; Wasserscheid, P. Liquid organic hydrogen carriers (LOHCs): toward a hydrogen-free hydrogen economy. *Acc. Chem. Res.* **2017**, *50*, 74.
- (6) Markiewicz, M.; Zhang, Y. Q.; Bösmann, A.; Brückner, N.; Thöming, J.; Wasserscheid, P.; Stolte, S. Environmental and health impact assessment of Liquid Organic Hydrogen Carrier (LOHC) systems—challenges and preliminary results. *Energy Environ. Sci.* **2015**, *8*, 1035.
- (7) Teichmann, D.; Arlt, W.; Wasserscheid, P.; Freymann, R. A future energy supply based on Liquid Organic Hydrogen Carriers (LOHC). *Energy Environ. Sci.* **2011**, *4*, 2767.
- (8) Palo, D. R.; Dagle, R. A.; Holladay, J. D. Methanol steam reforming for hydrogen production. *Chem. Rev.* **2007**, *107*, 3992.
- (9) Liu, W.-C.; Baek, J.; Somorjai, G. A. The Methanol Economy: Methane and Carbon Dioxide Conversion. *Top. Catal.* **2018**, *61*, 530.
- (10) Greely, J.; Mavrikakis, M. Competitive paths for methanol decomposition on Pt (111). *J. Am. Chem. Soc.* **2004**, *126*, 3910.
- (11) Kuhn, J. N.; Huang, W.; Tsung, C.-K.; Zhang, Y.; Somorjai, G. A. Structure Sensitivity of Carbon-Nitrogen Ring Opening: Impact of Platinum Particle Size from below 1 to 5 nm upon Pyrrole Hydrogenation Product Selectivity over Monodisperse Platinum Nanoparticles Loaded onto Mesoporous Silica. *J. Am. Chem. Soc.* **2008**, *130*, 14026.
- (12) Tsung, C. K.; Kuhn, J. N.; Huang, W. Y.; Aliaga, C.; Hung, L. I.; Somorjai, G. A.; Yang, P. D. Sub-10 nm platinum nanocrystals with size

and shape control: catalytic study for ethylene and pyrrole hydrogenation. *J. Am. Chem. Soc.* **2009**, *131*, 5816.

(13) Qiao, B.; Wang, A.; Yang, X.; Allard, L. F.; Jiang, Z.; Cui, Y.; Liu, J.; Li, J.; Zhang, T. Single-atom catalysis of CO oxidation using Pt<sub>1</sub>/FeOx. *Nat. Chem.* **2011**, *3*, 634.

(14) Lin, L.; Zhou, W.; Gao, R.; Yao, S.; Zhang, X.; Xu, W.; Zheng, S.; Jiang, Z.; Yu, Q.; Li, Y. W.; Shi, C.; Wen, X. D.; Ma, D. Low-temperature hydrogen production from water and methanol using Pt/ $\alpha$ -MoC catalysts. *Nature* **2017**, *544*, 80.

(15) Liu, P.; Zhao, Y.; Qin, R.; Mo, S.; Chen, G.; Gu, L.; Chevrier, D. M.; Zhang, P.; Guo, Q.; Zang, D.; Wu, B.; Fu, G.; Zheng, N. Photochemical route for synthesizing atomically dispersed palladium catalysts. *Science* **2016**, *352*, 797.

(16) Yang, X. F.; Wang, A. Q.; Qiao, B. T.; Li, J.; Liu, J. Y.; Zhang, T. Single-atom catalysts: a new frontier in heterogeneous catalysis. *Acc. Chem. Res.* **2013**, *46*, 1740.

(17) Chen, Y.; Ji, S.; Chen, C.; Peng, Q.; Wang, D.; Li, Y. Single-atom catalysts: synthetic strategies and electrochemical applications. *Joule* **2018**, *2*, 1242.

(18) Nie, L.; Mei, D.; Xiong, H.; Peng, B.; Ren, Z.; Hernandez, X.; DeLaRiva, A.; Wang, M.; Engelhard, M. H.; Kovarik, L.; Datye, A. K.; Wang, Y. Activation of surface lattice oxygen in single-atom Pt/CeO<sub>2</sub> for low-temperature CO oxidation. *Science* **2017**, *358*, 1419.

(19) Chen, J.; Wanyan, Y.; Zeng, J.; Fang, H.; Li, Z.; Dong, Y.; Qin, R.; Wu, C.; Liu, D.; Wang, M.; Kuang, Q.; Xie, Z.; Zheng, L. Surface Engineering Protocol To Obtain an Atomically Dispersed Pt/CeO<sub>2</sub> Catalyst with High Activity and Stability for CO Oxidation. *ACS Sustainable Chem. Eng.* **2018**, *6*, 14054.

(20) Rioux, R. M.; Song, H.; Hoefelmeyer, J. D.; Yang, P.; Somorjai, G. A. High-surface-area catalyst design: synthesis, characterization, and reaction studies of platinum nanoparticles in mesoporous SBA-15 silica. *J. Phys. Chem. B* **2005**, *109*, 2192.

(21) Aliaga, C.; Park, J. Y.; Yamada, Y.; Lee, H. S.; Tsung, C. K.; Yang, P. D.; Somorjai, G. A. Sum frequency generation and catalytic reaction studies of the removal of organic capping agents from Pt nanoparticles by UV–ozone treatment. *J. Phys. Chem. C* **2009**, *113*, 6150.

(22) Kappers, M. J.; van der Maas, J. H. Correlation between CO frequency and Pt coordination number. A DRIFT study on supported Pt catalysts. *Catal. Lett.* **1991**, *10*, 365.

(23) Gibson, K. D.; Dubois, L. H. Step effects in the thermal decomposition of methanol on Pt (111). *Surf. Sci.* **1990**, *233*, 59.

(24) Greeley, J.; Mavrikakis, M. A first-principles study of methanol decomposition on Pt (111). *J. Am. Chem. Soc.* **2002**, *124*, 7193.

(25) Desai, S. K.; Neurock, M.; Kourtakis, K. A periodic density functional theory study of the dehydrogenation of methanol over Pt (111). *J. Phys. Chem. B* **2002**, *106*, 2559.

(26) Wiebenga, M. H.; Kim, C. H.; Schmieg, S. J.; Oh, S. H.; Brown, D. B.; Kim, D. H.; Lee, J. H.; Peden, C. H. F. Deactivation mechanisms of Pt/Pd-based diesel oxidation catalysts. *Catal. Today* **2012**, *184*, 197.

(27) Mao, M.; Lv, H.; Li, Y.; Yang, Y.; Zeng, M.; Li, N.; Zhao, X. Metal Support Interaction in Pt Nanoparticles Partially Confined in the Mesopores of Microsized Mesoporous CeO<sub>2</sub> for Highly Efficient Purification of Volatile Organic Compounds. *ACS Catal.* **2016**, *6*, 418.

